Follow-Up Observations of Faint Short-Period Variable Stars

McKenna Myckowiak

A senior thesis submitted to the faculty of
Brigham Young University
in partial fulfillment of the requirements for the degree of

Bachelor of Science

Eric G. Hintz, Advisor

Department of Physics and Astronomy

Brigham Young University

ABSTRACT

Follow-Up Observations of Faint Short-Period Variable Stars

McKenna Myckowiak
Department of Physics and Astronomy, BYU
Bachelor of Science

The Asteroid Terrestrial-impact Last Alert System, also known as ATLAS, is a survey meant to find potentially dangerous asteroids that could cause life threatening destruction to Earth. The survey consists of four telescopes, mostly located in the southern hemisphere, that scan the whole sky several times per night looking for objects that change in position, magnitude or both. Although the ATLAS survey is designed to detect asteroids, it also happens to be successful at finding variable stars due to continuous monitoring of the night sky. In my thesis, I analyze five Delta Scuti variable stars that ATLAS has detected. Since the ATLAS telescopes are not designed to find variable stars, the stars that ATLAS classifies as variable stars may not actually be variable stars. The purpose of my project is to determine the accuracy of the ATLAS survey. I do this taking raw data from the Dominion Astrophysical Observatory's 1.8 meter Plaskett telescope and perform image reduction/analysis to find pulsation periods for each of the ATLAS objects I received data for. Then, I come to a conclusion about the ATLAS survey's accuracy and the need for more data so that future variable star models can be as accurate as possible.

Keywords: ATLAS Survey, MATLAS, δ Scuti, Variable Stars, Pulsation Period

ACKNOWLEDGMENTS

I would like to express my gratitude for Dr. Hintz and all that he has done for me at BYU. It is because of him that I have been able to do this research and have this great experience. I would also like to thank my parents. My father, not only for the financial support he has given me but for also making me want to be more loving, thoughtful and giving to those around me. My mother, not only for guiding me through problems I wish I would never have to face, but for also being my best friend. Without their love and support, I wouldn't be able to be 1500 miles away from them.

Contents

Chapter 1

Introduction

1.1 The Hertzsprung-Russell Diagram

The Hertzsprung-Russell Diagram [1], also known as the H-R Diagram, demonstrates the easiest way to classify stars. With surface temperature on the x-axis and luminosity on the y-axis, the correlation between different types of stars is evident. Classifying stars from brown dwarfs to supergiants, the H-R Diagram provides basic information about not only the surface temperature and luminosity of various stars but also shows the inevitable end-of-life stages for each type of star.

In Figure 1.1, the Main Sequence shows a correlation between surface temperature and luminosity. As the surface temperature increases, the luminosity increases. Figure 1.2 shows the Mass-Luminosity Relation, which shows that as the luminosity increases, the mass increases. The different values for alpha imply that the relationship between mass and luminosity is non-linear which can be seen in Figure 1.1 as the Main Sequence is not a linear line. The Main Sequence is where stars live most of there lives.

At the end-of-life stage for each star, the mass of the core determines whether a star will end up as a White Dwarf, Neutron Star or Black Hole. Masses of the core less than 1.4 Solar Masses (which

is a commonly used unit of measurement; 1 Solar Mass = the mass of the Sun) will eventually turn into a White Dwarf. Masses greater than 1.4 Solar Masses and smaller that 3 Solar Masses will eventually turn into a Neutron Star and masses greater than 3 Solar Masses will eventually turn into a Black Hole. Figure 1.3 shows the life stages of stars with different masses.

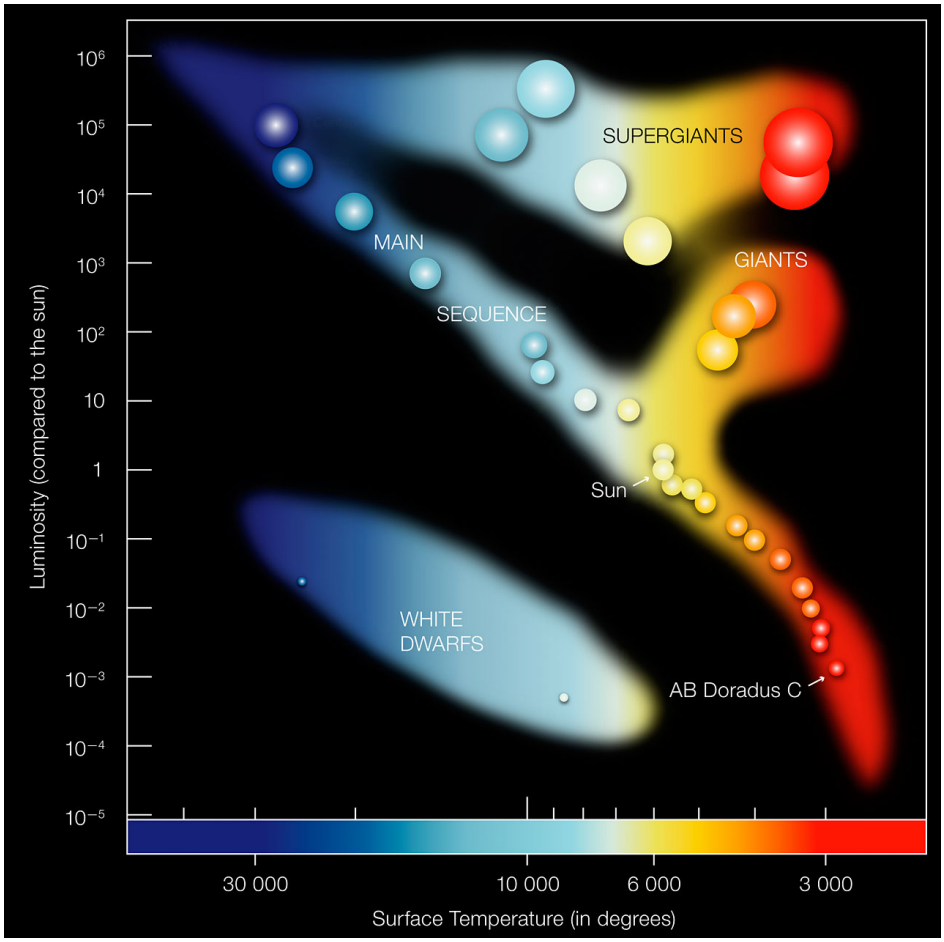

Figure 1.1 The H-R Diagram, showing the classification of stars

$$\frac{L}{L_\odot} = \left(\frac{M}{M_\odot}\right)^\alpha$$
$$M \lesssim 0.3M_\odot : \ \alpha \approx 1.8$$
$$0.3M_\odot \lesssim M \lesssim 3M_\odot : \ \alpha \approx 4.0$$
$$3M_\odot \lesssim M : \ \alpha \approx 2.8$$

Figure 1.2 Mass-Luminosity relation

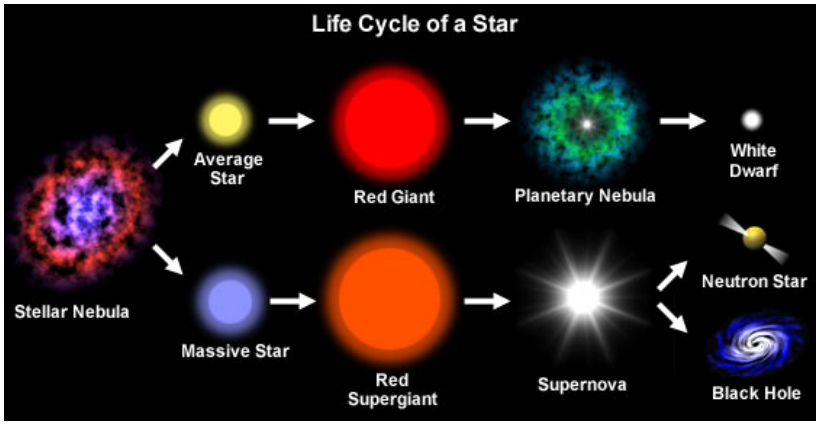

Figure 1.3 The three main life stages of stars on the Main Sequence

1.2 The Instability Strip and Types of Variable Stars

The Instability Strip is a area on the H-R Diagram, that intersects the Main Sequence, and is the place where variable stars reside. Figure 1.4 gives a rough estimate of where the Instability Strip intersects the Main Sequence. Stars that have lived on the Main Sequence for most of their lives may enter the Instability Strip multiple times on their way towards their end-of-life stage. The Instability Strip is named for the instability of the outer layers of the stars that reside there. As stated earlier, the mass of the core of each star determines the end of life stage for that star. During the period between leaving the Main Sequence and becoming a Neutron Star, White Dwarf or Black Hole, a star must shed its outer layers. To do this, instability in the outer layers must happen. To the observer, a star passing through the instability strip will vary in luminosity and temperature. This variation in luminosity and temperature can be regular and periodic or can be irregular. Variable

stars in the Instability Strip generally pulsate due to He II (liquid form of Helium) layer transforming into a He III (the fully ionized state of Helium) layer. The He III layer is closer to the core, meaning it is hotter, than the He II layer because a higher temperature, which correlates to more energy, is needed to ionize the helium atoms.

All matter tends towards an equilibrium. This principle is what continuously drives the expansion and contraction of these stars. As the star contracts, the temperature increases and He II turns into He III. The star's absolute magnitude, a measurement of the luminosity of the object in dimensionless units, and apparent magnitude, the brightness of the object as seen in the night sky, both change due to these processes. The measurements of magnitude is counter intuitive, meaning that the smaller the magnitude the brighter the object and vice versa. As the star contracts, the temperature and density increases and the absolute magnitude, and thus the apparent magnitude, decreases. The He II layer starts to transform to He III due to the increase in temperature. As the temperature increases, the star will start to expand. As the star expands, the temperature and density decrease and the He III layer recombines back into He II. The absolute and apparent magnitude of the object increases, meaning the luminosity of the star decreases. This is a general example of the processes that cause variability in variable stars. However there are many different types of variable stars.

1.2.1 Long-Period Variables

Long-Period Variables [2] describe a group of variable stars with periods longer than 100 days, some even exceeding 1000 days. These types of variable stars are difficult to observe due to their long period cycle. Though periods of these types of stars have been found, some stars with variations in magnitude leave astronomers to believe they are periodic when they are not. By the mid 1900s, astronomers discovered that stars denoted as long-period variables were almost always cool giant or supergiant stars.

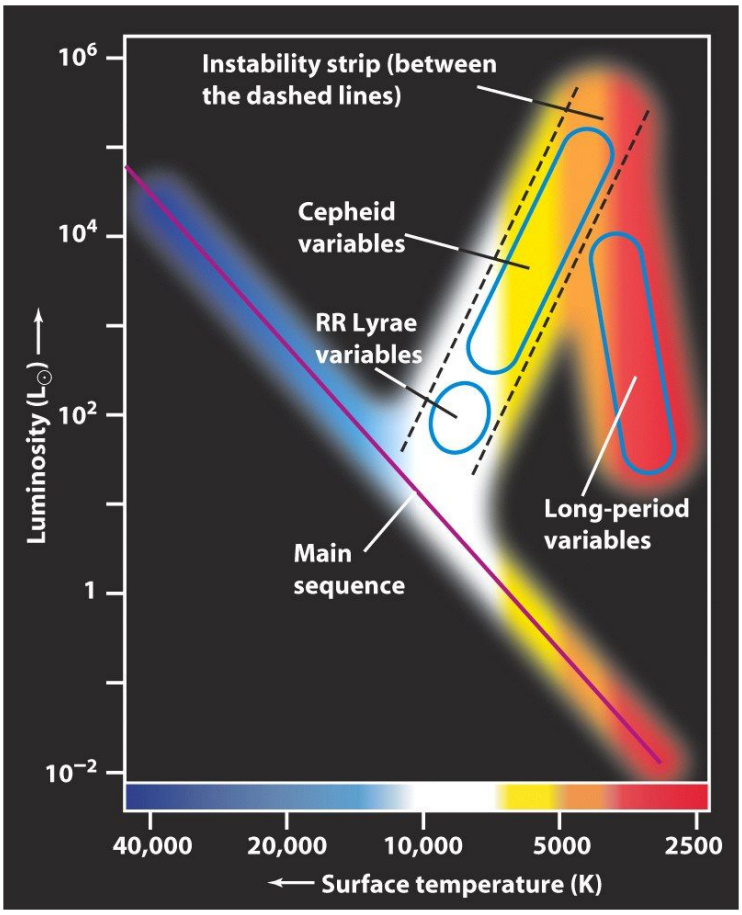

Figure 1.4 A rough example of where the Instability Strip crosses the Main Sequence

1.2.2 RR Lyrae variables

RR Lyrae variables [3] are variable stars usually found in globular clusters. They are about half the mass of the Sun with periods less than a day. These stars are in their final end-of-life stages. They are stars that were on the Main Sequence, evolved into a Red Giant star where they eventually shed mass to become a RR Lyrae variable. These variables are metal-poor meaning that they are some of the oldest stars in the universe.

1.2.3 Cepheid variables

Cepheid variables [4] are periodic stars that vary radially, meaning they change diameter and brightness during their pulsation period. It strongly correlates to the Period-Luminosity relation, meaning that an accurate change in luminosity will give an accurate pulsation period. There are many types of Cepheid stars, the most common are Classic Cepheids and Type II Cepheids. Classic Cepheids have periods from days to months. They are between 4 and 20 Solar Masses and 10,000 times more luminous than the Sun. Classic Cepheids are metal-rich meaning that they are some of the youngest stars in the universe. Type II Cepheids have periods between 1 and 50 days and are about half the mass of the Sun. Type II Cepehids are metal-poor meaning that they are some of the oldest stars in the universe.

1.3 δ Scuti Stars

δ Scuti [5] stars are Cepheid-like stars, sometimes even called dwarf Cepheids. They are similar to Cepheid variables such that they pay strict heed to the Period-Luminosity relation, meaning a more accurate luminosity leads to a more accurate period. δ Scuti variables pulsate in radial modes, much like Cepheid stars, and non-radial modes. Non-radial modes are pulsations where different parts of the star move inward and outward at the same time, thus not conforming to their spherical equilibrium state. Radial modes are pulsation cases where the star pulsates around their equilibrium state. Both modes lead variable stars to change in shape which leads to a change in temperature and, thus, a change in luminosity. δ Scuti stars have periods on the order of a couple of hours. δ Scuti stars differ from Cepheid variables in that they lie closer to the Main Sequence, as seen in Figure 1.5.

My research revolves around observing δ Scuti stars that have already been discovered, characterized and observed by the ATLAS survey. The ATLAS survey categorizes astronomical objects

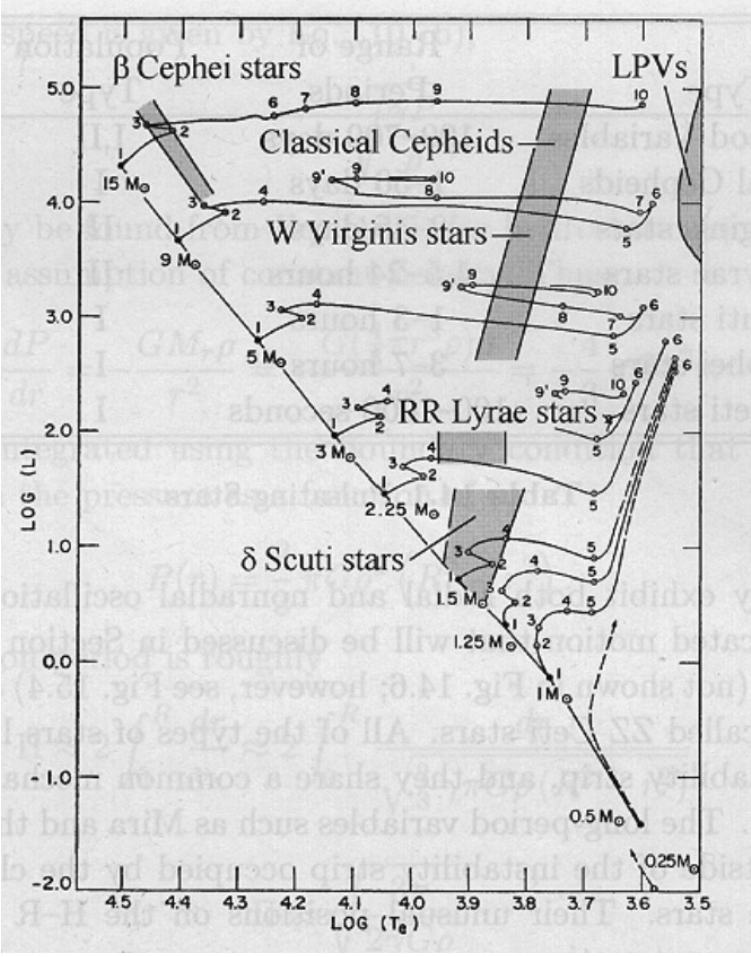

Figure 1.5 A rough example of where the δ Scuti variables lie on the Instability Strip

that lie within a certain region of the sky. The ATLAS survey has already taken observations of certain δ Scuti stars and has found their pulsation period. I analyze recent observations of these stars and compare my observed periods with the periods that have already been published by the ATLAS survey. The main purpose of this is to double check whether the ATLAS Survey calculations are correct. The more accurate the available data is, the more accurate future models of these stars will be.

Chapter 2

Methods

2.1 ATLAS Survey

The Asteroid Terrestrial-impact Last Alert System, also known as ATLAS, is a survey designed to find and catalogue asteroids that could potentially harm Earth. The ATLAS Project is funded by NASA and operated through the University of Hawaii. Four telescopes, two located in Hawaii, one located in South Africa and another in Chile, each scan a different quarter of the night sky in search of asteroids. To search for asteroids, each telescope searches for objects that differ in magnitude and position. Depending on the size of the asteroid, ATLAS will give a warning time as to when the asteroid is believed to hit Earth, so that affected areas can be evacuated. Relatively large asteroids will be found further away from Earth, while smaller asteroids will be found closer to Earth. Although the ATLAS telescopes are exceptional at finding asteroids, many astronomical objects differ in magnitude and position. So far, the ATLAS Project has found 935 Near-Earth Asteroids, 93 Potentially Hazardous Asteroids, 81 Comets and 16,191 Supernovae. Along with these objects, ATLAS has found numerous pulsating variable stars. All of these objects were catalogued in the ATLAS Survey.

Each object is classified a certain way. Pulsating variable stars with one period are denoted with the word ATLAS and a number. For example, ATLAS75 is a pulsating variable star with a single period. The number 75 is a number given to signify the magnitude relative to other pulsating variable stars. This does not mean that ATLAS75 has a magnitude of 75. Lower numbers, like 75, are brighter and have a smaller magnitude while higher numbers, like 818, are very faint and have a higher magnitude. Pulsating variable stars with multiple periods are denoted with MATLAS and a number. The number means the same as the ATLAS objects and M denotes a variable star with multiple periods. The objects analyzed in this paper are ATLAS388, ATLAS411, ATLAS734, MATLAS545 and MATLAS564.

2.2 Dominion Astrophysical Observatory

The Dominion Astrophysical Observatory (DAO) is an observatory located in British Columbia. It was funded by the Canadian government and was built in 1918. It houses two research telescopes, the main attraction being the 1.8-meter Plaskett Telescope which was proposed in 1910 and finished when the observatory opened, in 1918. DAO was one of the most famous astrophysical centers up until the 1960s when other bigger and newer observatories were made. The Plaskett Telescope is an ideal instrument to observe faint pulsating variable stars due to its large 1.8-meter mirror which is more sensitive to light than smaller mirrors. To calculate an accurate period for each faint short period variable star, we need to find an accurate change in magnitude as the star pulsates. The larger the mirror used in our observations, the more accurately we can find the difference in magnitude for these faint objects. This is why we used the 1.8-meter Plaskett Telescope for our observations.

Observations for approximately 15 pulsating variable stars were taken in the year 2020 at DAO. These CCD images were sent to Dr. Hintz at Brigham Young University where I was given the task to reduce the CCD images and find a period for each object. As mentioned before, objects

presented in this paper are ATLAS388, ATLAS411, ATLAS734, MATLAS545 and MATLAS564.

Figure 2.1 The 1.8-meter Plaskett Telescope at the Dominion Astrophysical Observatory in British Columbia. On the left, the Plaskett Telescope in 1918. On the right, the Plaskett Telescope in 2018.

2.3 Image Reduction

When CCD images are taken by a telescope, there are certain aberrations in each image that needs to be corrected so accurate data can be taken. These aberrations can be corrected by taking calibration frames each night before observation and applying them to object frames during the image reduction process. In general, there are three different types of calibration frames; Zeros (or Bias), Darks and Flats. In my project I only use Zeros (Bias) or Flats due to the faintness of my target stars. Each calibration frame serves a purpose that is useful. Zeros (or Bias) frames are zero exposure (no light falling on the CCD) CCD images used to capture the different read-out noise of each pixel in the CCD sensor. This read-out noise is a byproduct of manufacturing. When looking at a Zero (or Bias)

frame there seems to be no read-out noise, but we still take them because we want our observations to be as precise as possible. Multiple Zero (or Bias) frames are taken at the beginning of each observation night. An average of the Zero (or Bias) frame is produced by the image reduction program we use, called IRAF (Image Reduction and Analysis Facility), to create a master Zero (or Bias) frame called a Zeros.fits file or Bias.fits file. This master file is then applied to all of the other images that were taken that night, including the Dark and Flat frames. Figure 2.2 is an example of a Zero frame.

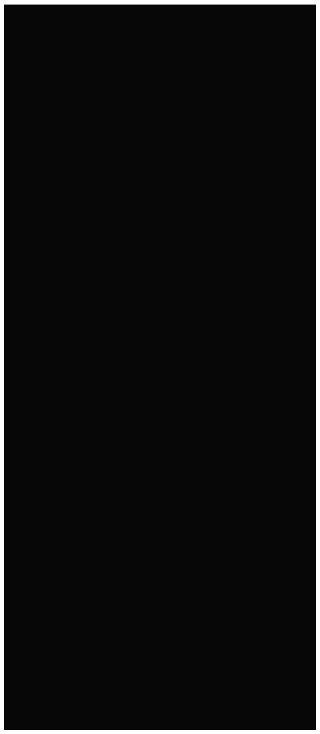

Figure 2.2 An example of a Zero frame

Next we would apply the Dark frames. When taking an exposure, thermal noise (also known as white noise) becomes present on the CCD images. Thermal noise is present because we are using electricity to keep the CCD at a very cold temperature (usually between 223 to 173 Kelvin or, in everyday terms, -58 to -148 degrees Fahrenheit). The longer the exposure, the more photons are collected in the pixels. The thermal noise comes from these pixels and can cause small aberrations

on the CCD images. Dark calibration frames measure the thermal noise on the CCD. Usually 3-5 dark frames are taken. We then create a master Dark file by averaging out the thermal noise onto one frame called a Dark.fits file. Due of the faintness of the objects I will be presenting, dark frames are not taken because we need to collect all of the photons we can from these objects. Taking away thermal noise might take away some of the photons that are desperately needed to find the magnitude of each target star and their corresponding comparison stars. So, dark frames are not taken and not applied due to the small amount of photons that are captured from these objects.

After we apply the Zero.fits, we apply the Flat.fits. Mirrors on telescopes are not cleaned due to the potential of scratches that can cause inaccuracy in our observations. So, dust is collected on the mirror. Light exposure from everyday life also affects our images. So, to take dust marks and light exposure out of the object frames, we take flat images which show these aberrations. Then we take an average of the dust and light exposure images by creating a Flat.fits image. Then we subtract this image from the rest of the object frames. Now we have object frames that have no aberrations on them and that are ready to be used to find a pulsation period. Image reduction was preformed on all object frames that were used to calculate the period and magnitude of each object presented in this paper. Figure 2.3 shows an example of a flat frame.

2.4 AstroImageJ

AstroImageJ is a program that we use to determine how the object's magnitude changes throughout the night. This is preformed by picking non-saturated comparison stars that are present in all frames and tracking how the target star changes relative to those comparison stars. At this point in my research, I make an important assumption that makes it possible to find the magnitude and period of each object. We assume that all the light from the stars, other than the object star (also known as the target star), are relatively constant. We use a coordinate finder program, called SIMBAD, which

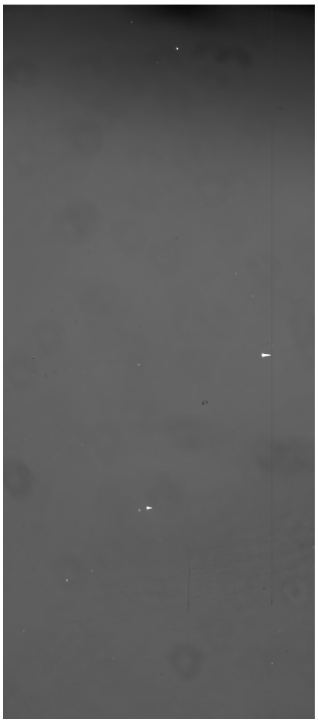

Figure 2.3 An example of a flat frame

helps us to find the magnitude of comparison stars that are present in each object frame. This takes some trial and error. We try to find as many comparison stars on SIMBAD that are located in the frame and have a magnitude attached to them. This can be tricky as not all usable comparison stars have an attached magnitude. Nevertheless, we use a combination of stars with attached magnitudes and stars that don't have attached magnitudes. As long as there is one comparison star that has an attached magnitude, AstroImageJ calculates the magnitude of the target star as it varies throughout the night. That is how we get a magnitude for the target star, next we need to use the magnitude of the target star to find the frequency that the target star pulsates at.

Figure 2.4 shows an example of an object frame with no attached magnitudes. The green circle encloses the target star while the red circles enclose the comparison stars that I choose for this object. As stated earlier, not all object frames have stars with attached magnitudes in them. That means without a relative magnitude, AstroImageJ won't calculate a magnitude for the target star. This has

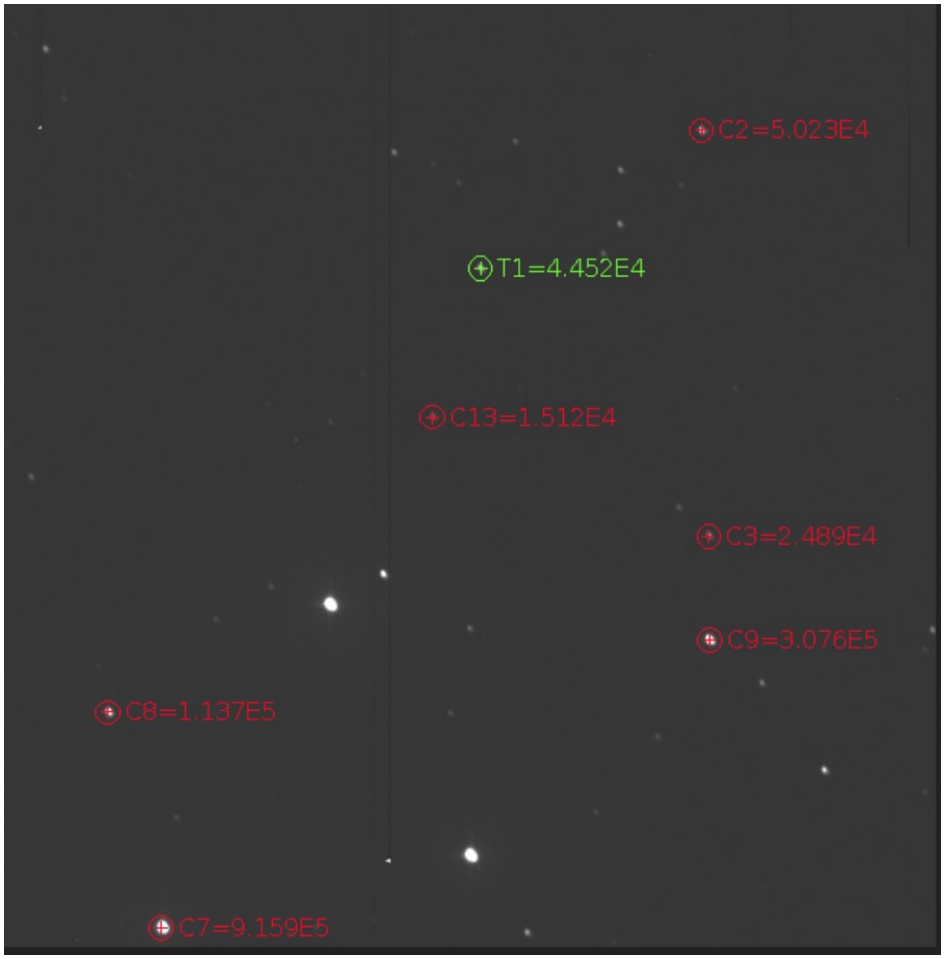

Figure 2.4 An example of an object frame with no attached magnitudes.

happened to a number of stars that I have observed. Target stars that do not have comparison stars with an attached magnitude can be observed and a period can be found but it would take more time and have a higher chance of inaccuracy. Above I mentioned that non saturated stars are elected as usable comparison stars. This is another obstacle that we must work around. Comparison stars that are saturated are not usable because the magnitude of the comparison star as found on SIMBAD does not accurately represent the magnitude of the comparison star as present on the object frames. Saturation means that too many photons are being collected from one object. With saturation, photons will fill up pixel wells and overflow into other pixels in the CCD sensor. These stars are unusable and frames that have too much saturation are also unusable. Saturation can be prevented by limiting light exposure. However, my project is to observe and find a period for faint stars meaning I need a longer exposure time to collect as much light from these faint stars as possible. This poses a problem when my faint target stars are next to a very bright object. Saturated comparison stars are more common on really faint objects, like ATLAS818 and ATLAS885. Along with giving a magnitude of the target star, AstroImageJ also calculates a light curve.

Figure 2.5 gives a light curve of ATLAS388 from AstroImageJ. The x-axis is time (in Geocentric Julian Date) and the y-axis is relative flux (meaning the flux calculated relative to the comparison stars in the frame). The dotted blue line is the relative flux of the target star throughout the night. As you can see, the relative flux of the target star varies throughout the night. From this graph alone, we can see that this target is a pulsating variable star. The pink, salmon, red and orange dotted lines are the relative flux of the comparison stars throughout the night. The comparison stars are not exactly a straight line but we use them to calculate the variability of the target star because they are relatively constant compared to the target star. This method will give us the most accurate magnitude of the target star as it varies throughout the night. The yellow dotted line gives the airmass as the night progresses. This tracks the mass of the air along the line of sight of the star in the Earth's atmosphere. This data is automatically placed in the header at the time of observation

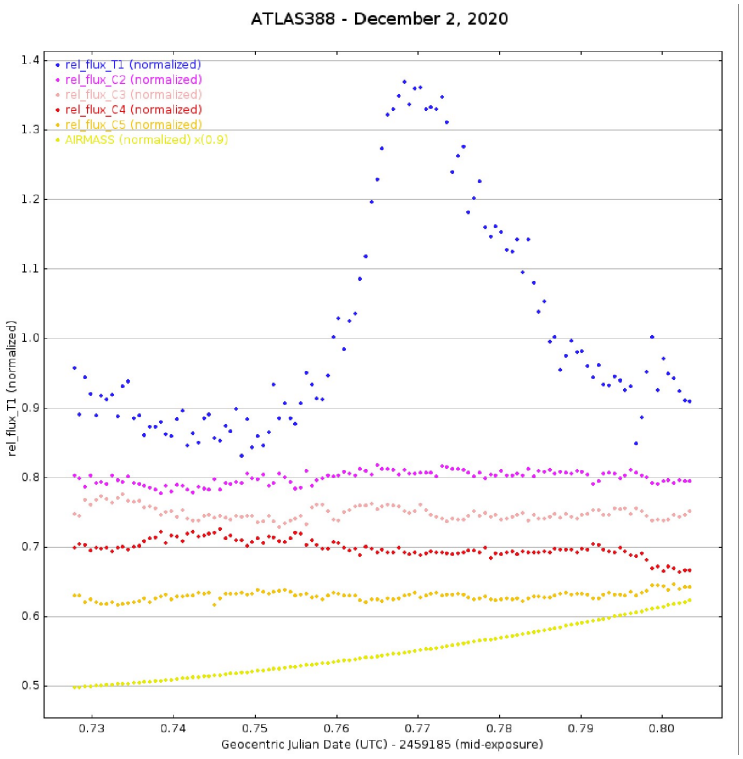

Figure 2.5 An example of a light curve of ATLAS388 from AstroImageJ (with data taken on December 2, 2020)

(each frame has a header which details multiple things like RA and DEC of the telescope, CCD temperature, pixel count, name of the telescope, owner of the images, etc.).

2.5 Period04

After finding how the magnitude of the target star changes throughout the night, we are ready to use Period04. Period04 is the last program we use and we use it to find the frequency and, therefore, the period of pulsation for the star. First, we open a text editor and input the time and magnitude change for the target star. We do this for all the observation nights of the target star. We then input these .txt files into Period04. Table 2.1 gives an example of the information that we input into Period04.

Period04 recognizes the time and magnitude of the star. We use Period04's Fourier decomposition function to calculate the frequency, amplitude and phase of pulsation. We also calculate the residuals from the main calculation, as the Fourier calculation can not use all the data to find a perfect formula that fits our light curves. Once we completed all of the calculations, Period04 gives us a phase diagram and a Fourier diagram. The phase diagram shows the Fourier fit using our .txt files. The more Fourier calculations we have, the more true the phase diagram will be to the pulsation of the star. The Fourier diagram shows the frequencies that are present in the star. We calculate the pulsation period from the fundamental frequency. Generally, delta Scuti stars have periods between 1 and 4 hours.

Table 2.1. Sample Period04 Input File.

Geocentric Julian Date (UTC)	Magnitude
2459087.92969	14.377503
2459087.93035	14.382540
2459087.93101	14.388410
2459087.93168	14.395158
2459087.93234	14.402463
2459087.93301	14.410482
2459087.93367	14.418835
2459087.93433	14.427547
2459087.93500	14.436660
2459087.93566	14.445741
2459087.93632	14.454828
2459087.93699	14.463958
2459087.93765	14.472697
2459087.93831	14.481088
2459087.93899	14.489158
2459087.93965	14.496522
2459087.94032	14.503338
2459087.94098	14.509284
2459087.94164	14.514404
2459087.94231	14.518698
2459087.94297	14.521960
2459087.94363	14.524232
2459087.94430	14.525495

Chapter 3

Results

3.1 Targets

For each of the five δ Scuti stars I observed, I created a light curve (of a specific night), a phase diagram and a Fourier diagram. In the sections below, I will present my findings on each star.

3.1.1 ATLAS388

ATLAS388 is one of the brighter objects that I did my research on. I had four nights of data. Once I had completed my image reduction, I plugged the CCD images into AstroImageJ. I got a magnitude for the target star and a light curve. Figure 3.1 shows a light curve that AstroImageJ gave from the night of October 25, 2020. Figure 2.5 gives a light curve of ATLAS388 from December 2, 2020. As stated before when talking about this object, that target seems quite variable compared to the comparison stars that I choose. The comparison stars were used on all the nights of data for ATLAS388. On October 25, 2020 the comparison stars are much more constant then they are for December 2, 2020. This could be for a number of reasons, the most probable was the CCD image quality was worse on December 2, 2020 than on October 25, 2020. This could be because there

was more light pollution in the sky on December 2, 2020 than on October 25, 2020 or the CCD was at a different temperature on December 2, 2020 than on October 25, 2020. Nonetheless, the small differences between the comparison stars of these two nights does not give too much of a difference on the magnitude of the target star. We combine all of the data into Period04 to give the best possible frequency and period of the target star. The average magnitude of the target star throughout the night was 14.3.

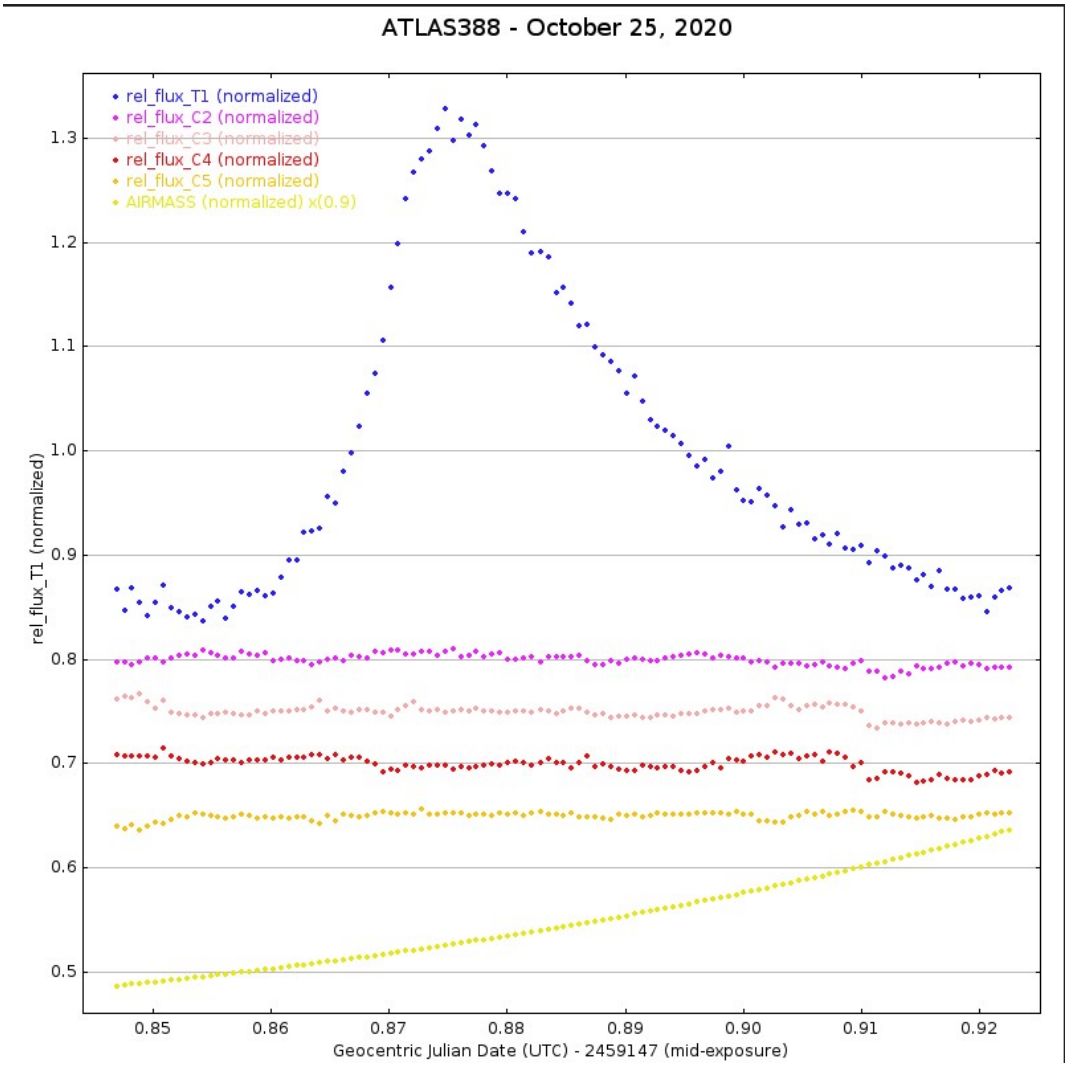

Figure 3.1 An example of a light curve of ATLAS388 from October 25, 2020

Figure 3.2 gives the phase diagram of ATLAS388. The different colors correspond to different nights. We have four nights, so we have four different colors. We can clearly see that ATLAS388 is variable because for each night, each dotted line goes up at the same time and goes down at the same time. There are some differences per night like how they don't all have the same amplitude, however the difference is very small. The green dotted line seems to differ from the rest of them and the blue dotted line seems to dip lower than the other colors. Even though we are taking observations of the same star, there are variations in the target's amplitude per night. The amplitude of the star simply means how the stars magnitude changes per night. The blue dotted line shows that the amplitude dips lower than the green dotted line.

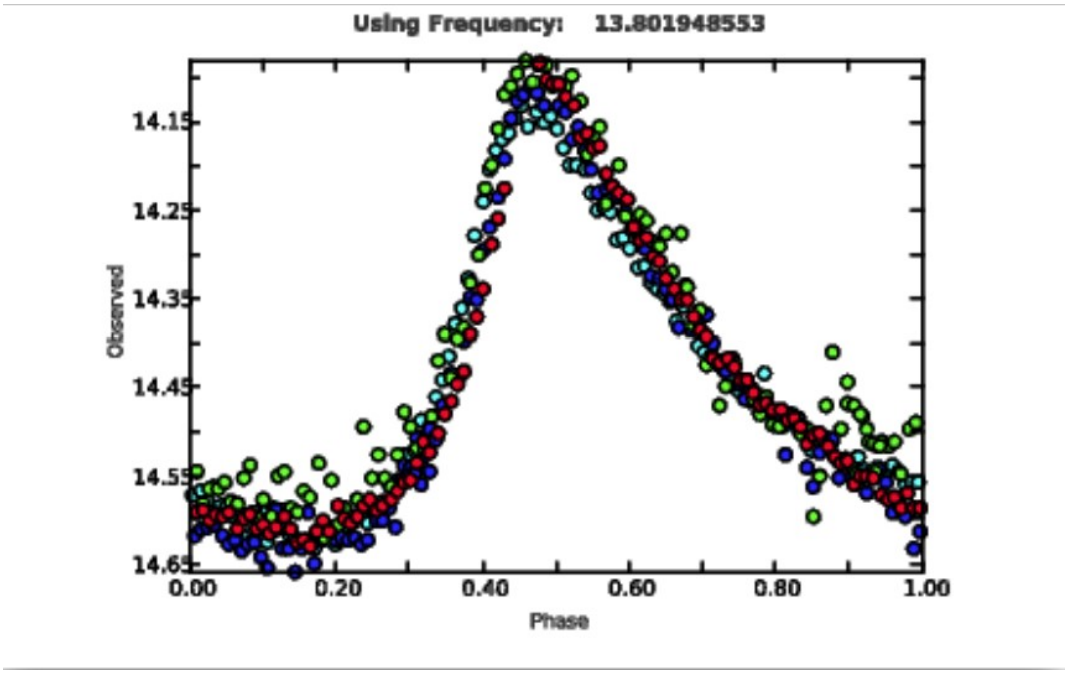

Figure 3.2 Phase diagram of ATLAS388

Figure 3.3 shows the Fourier graph of ATLAS388. The first maximum is the fundamental frequency, while the next is the first harmonic and the next is the second harmonic and so on. The purpose of the Fourier graph is to show that a pulsation is actually happening in the star. Some

process within the star is making this pulsation happen. We need to prove this to quell any doubts that this is not a variable star. From the frequency, we can perform a simple calculation to find the period of pulsation. We simply take the inverse of the frequency to get the period of pulsation in days. To better understand the period, we give the period in hours. The period of this star is 1.738 hours.

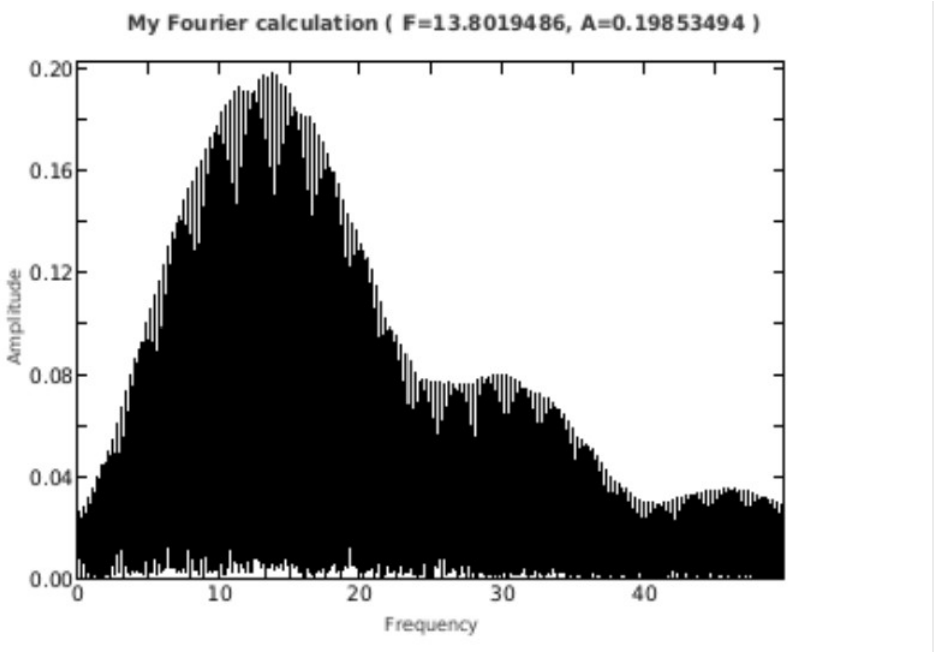

Figure 3.3 Fourier graph of ATLAS388

3.1.2 ATLAS411

ATLAS411 has an average magnitude of 14.69. After reducing all the CCD images for ATLAS411, I plugged the images into AstroImageJ and got the magnitude variation throughout the night and the light curves for the five nights ATLAS411 was observed. Figure 3.4 gives the light curve of ATLAS411 on August 25, 2020. Figure 3.5 gives the light curve of ATLAS411 on October 25, 2020. Like the light curves for ATLAS388, the x-axis is time while the y-axis is flux. The same

comparison stars were used for all the nights of data for ATLAS411. The light curve for August 25, 2020 shows the comparison stars being more variable than the light curve for October 25, 2020. The airmass is also quite different between the two nights, however the target for both of these nights hits the same flux. This is good and shows that we must be doing something right.

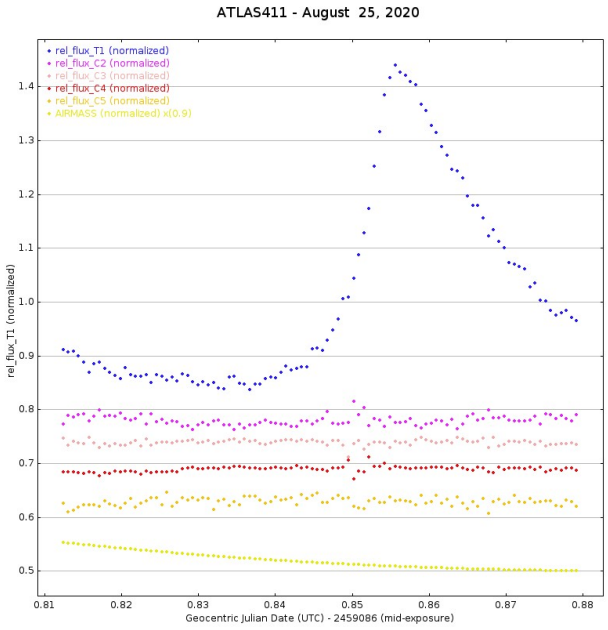

Figure 3.4 Light curve for ATLAS411 on August 25, 2020

Figure 3.6 gives the phase diagram for ATLAS411. There are certain differences between each night, however the differences are slight. The dark blue dotted line seems to have a different maximum than the rest of them, which is something to note about this star. Each dotted line hits the minimum and the maximum at the same time, so we can say that this star has a period. Figure 3.7 gives the Fourier diagram of ATLAS411. Again, we can see the fundamental frequency, the first harmonic and the second harmonic. This proves that there is some process within the star that is causing this pulsation. The period of this star is 1.77056 hours.

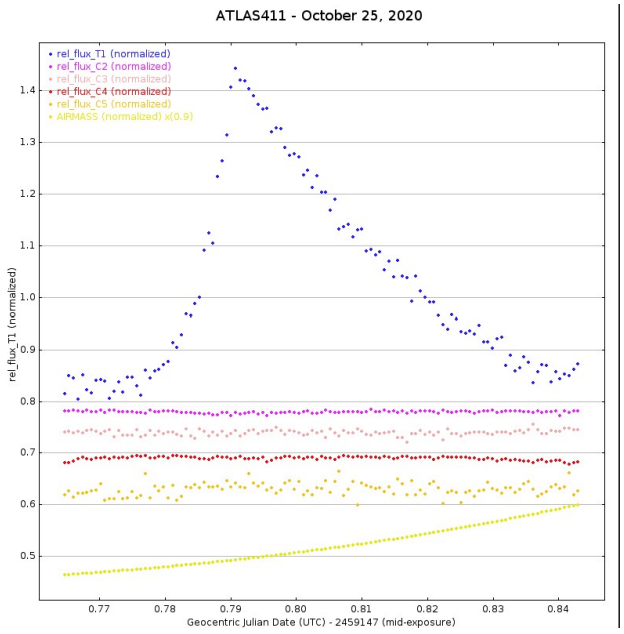

Figure 3.5 Light curve for ATLAS411 on October 25, 2020

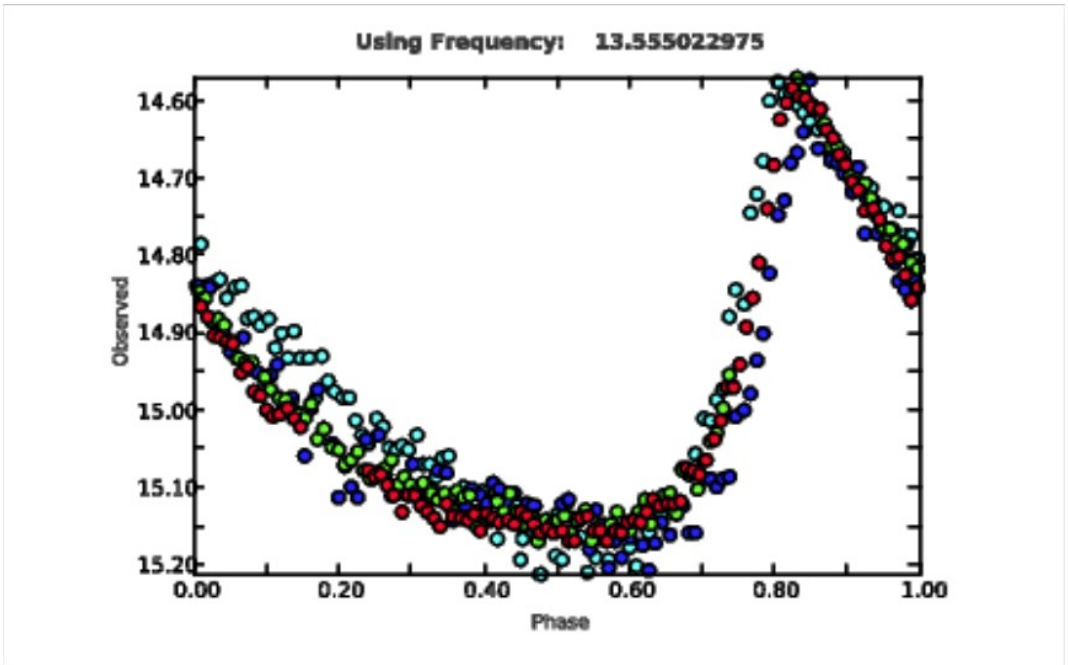

Figure 3.6 Phase diagram for ATLAS411

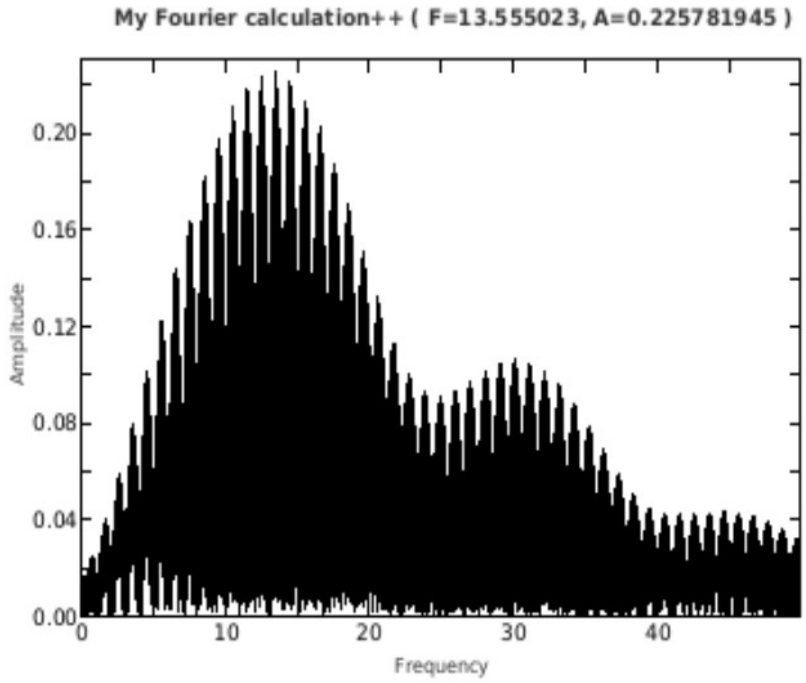

Figure 3.7 Fourier diagram for ATLAS411

3.1.3 MATLAS545

As mentioned before the MATLAS stars are multi periodic which will be apparent when we look at the phase diagram. The average magnitude for MATLAS545 is 14.3 mag. MATLAS545 was observed for three nights. After we reduce all the images for MATLAS545, we input our target frames into AstroImageJ. Figure 3.8 shows a light curve of MATLAS545 from April 17, 2020. The red dotted comparison star seems to be more variable than what is ideal, however it does have an magnitude attached and there were not many of those present on these frames. The salmon and yellow comparison stars seem mostly constant which is ideal. The airmass (pale yellow line) steadily grows throughout the night which is expected. The blue dotted target seems to be quite variable. On April 17, 2020 it seems that we got almost two full periods for this target. The more data that we have for an object, the more accurate our results will be, so it is great that we got almost two full periods.

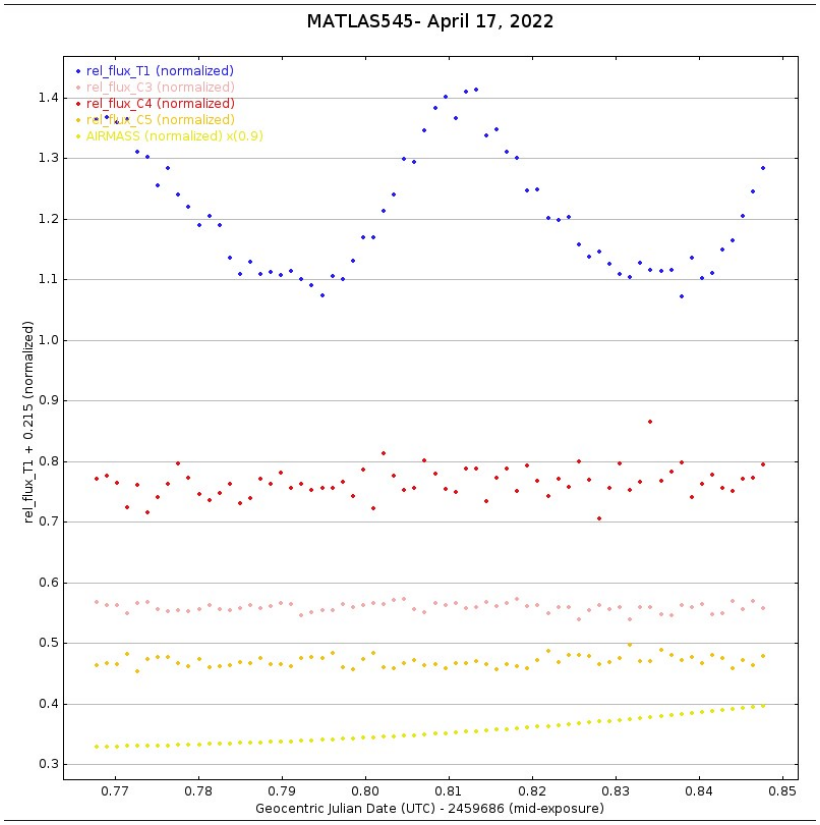

Figure 3.8 Light curve for MATLAS545 from April 17, 2020

Figure 3.9 gives the phase diagram for this object. The different amplitudes for all of the nights clearly shows that this is a multi periodic star. The different frequencies correlate to different amplitudes, but the period of the star can still be found, as we can see that although there is varying different types of amplitudes all the nights have a maximum and minimum at the same time. That is where we get the period from. Figure gives the Fourier diagram for MATLAS545. Again, this shows that there is some kind of process in the star that is causing this pulsation. The period for MATLAS545 is 1.037 hours.

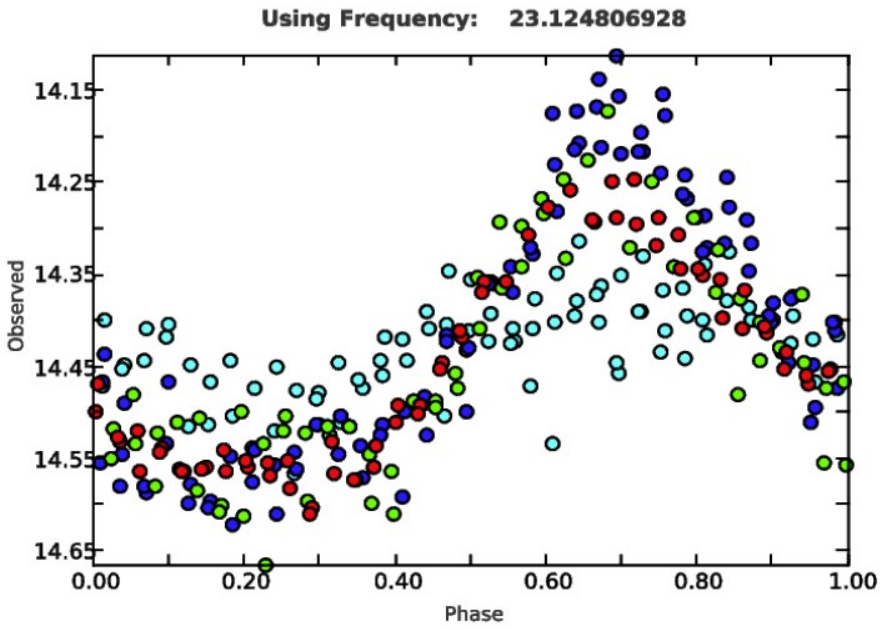

Figure 3.9 Phase diagram for MATLAS545

3.1.4 MATLAS564

MATLAS564 is another multi periodic star. MATLAS564 was observed for six nights. This is one of the targets I was given that had the most data available. As stated earlier, the more data available, the more accurate our results will be. Figure 3.10 gives the light curve of MATLAS564 from June 22, 2021. Figure 3.11 gives the light curve of MATLAS564 from July 29, 2021. The pink and yellow comparison stars lines for both nights seem to be quite constant, while the brown airmass steadily declines which is expected for both nights. The most interesting part of these two light curves is the difference between the target. On June 22, the flux is higher than on July 29. This is a clear indication, from the flux amplitude, that MATLAS564 is a multi periodic variable star.

Figure 3.12 shows the phase diagram for MATLAS564. We can see from this phase diagram that the amplitudes differ from night to night but all night have a maximum and minimum at the same time. This shows that this is a multi periodic variable stars with quite a few periods. However,

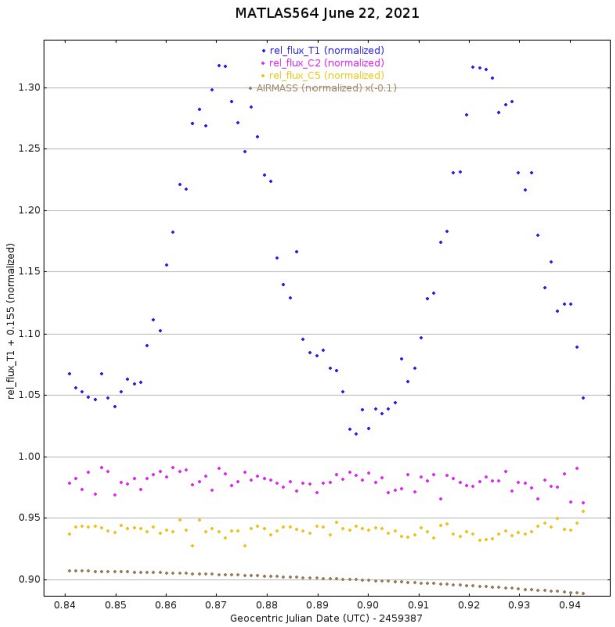

Figure 3.10 Light curve for MATLAS564 from June 22, 2021

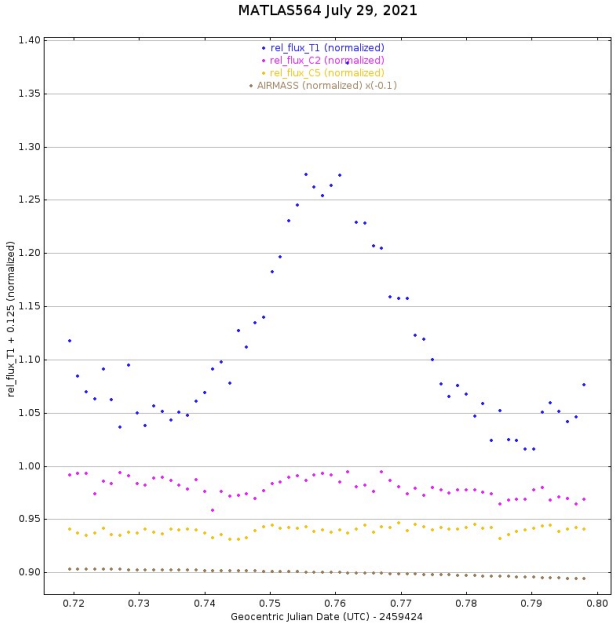

Figure 3.11 Light curve for MATLAS564 from July 29, 2021

no comparison stars with magnitudes could be found in the object frames. Even with that, we can still calculate a period from the main frequency that is given. The period for MATLAS564 is 1.359 hours.

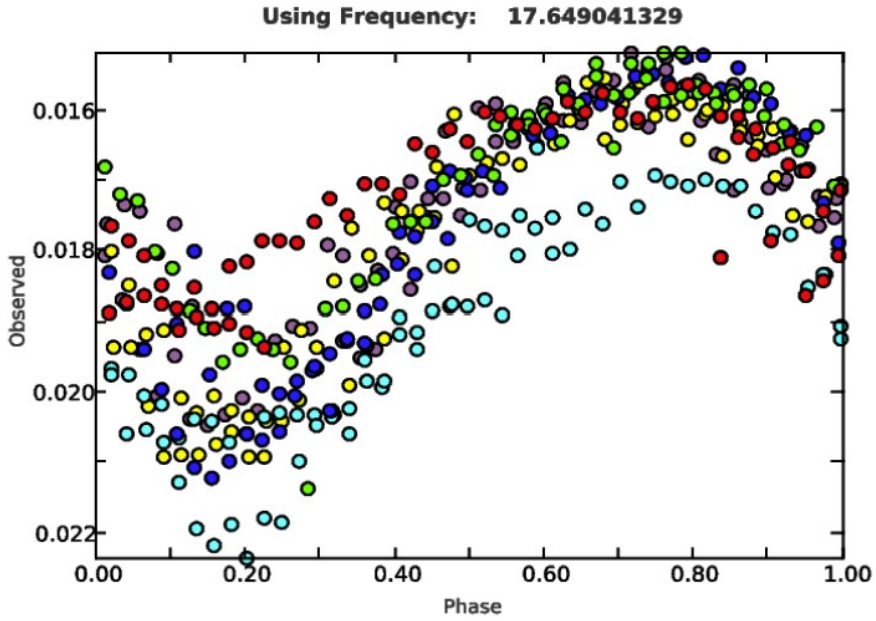

Figure 3.12 Phase diagram for MATLAS564

3.2 ATLAS734

ATLAS734 is the most interesting ATLAS object I have analyzed. The reason is ATLAS734 does not act the way that a single periodic variable star should. In fact, ATLAS734 acts more like a MATLAS object than an ATLAS object. This could be for any number of reasons for example, ATLAS734 may not a δ Scuti star or the ATLAS Survey wrongly categorized ATLAS734 as an ATLAS star rather than a MATLAS star. The one thing that we do know is that ATLAS734 is a variable star and that is shown on the Fourier Diagrams that will be presented in the next few sections. For this section, I look at each of the nights of observation in detail and provide evidence

which suggests that ATLAS734 is not an ATLAS object.

3.2.1 Light Curves

Figure 3.13 shows a light curve of ATLAS734 from July 8, 2020. Figure 3.14 shows a light curve of ATLAS734 from August 25, 2020. The pink, salmon, red and orange dotted lines are the comparison stars I used for all the four nights I had for ATLAS734. These comparison stars seem to be quite constant compared to the target star. The dotted yellow line representing airmass is what is expected. Like I said before, there are indications that this is not a single period variable star. The first indication that this star should not be an ATLAS object is the difference of flux from the two nights. The light curve form July 8, 2020 has a maximum flux of 1.32 and a minimum flux of 0.81, while the light curve from August 25, 2020 has a maximum flux of 1.24 and a minimum flux of 0.83. Next we look at the phase diagram of ATLAS734.

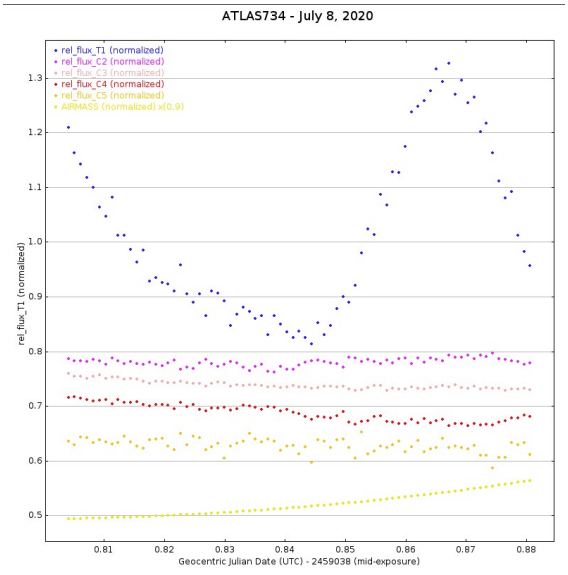

Figure 3.13 Light curve for ATLAS734 from July 8, 2020

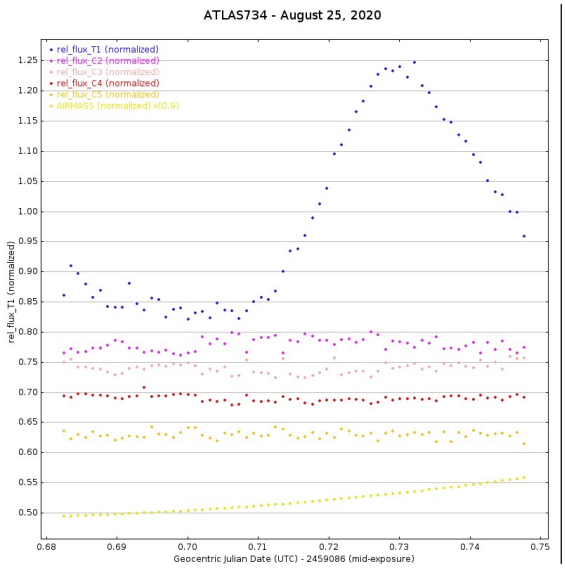

Figure 3.14 Light curve for ATLAS734 from August 25, 2020

3.2.2 Phase Diagrams

There are four usable nights of data for ATLAS734. I created five different phase diagrams so I could analyze this object deeper that I did the other ATLAS/MATLAS objects due to ATLAS734's initial inconsistencies. Figure 3.15 shows the phase diagram for ATLAS734. As you can see, the phase diagram for ATLAS734 looks different than the ones that we got for other ATLAS objects. This is another indication that ATLAS734 may not have been categorized correctly. The light blue line seems to cut off much faster than the other lines when coming off the maximum. Usually, layers of the star will ignite very quickly and cool off very slowly. We see this on the phase diagrams with a steep incline in brightness and a slow decline in brightness. The light blue line seems to indicate that the target cools off much faster that night than the other nights. However, the most interesting difference from other ATLAS phase diagrams is the dark blue dotted line. The dark blue line has a different minimum amplitude than the other three nights. Figure 3.15 has all four nights of data, the following four phase diagrams I introduce will have three nights of data. I did this in an attempt to see the affects that one night of data will have on the overall calculated period of ATLAS734. The

night with the obviously differing data was from July 8, 2020.

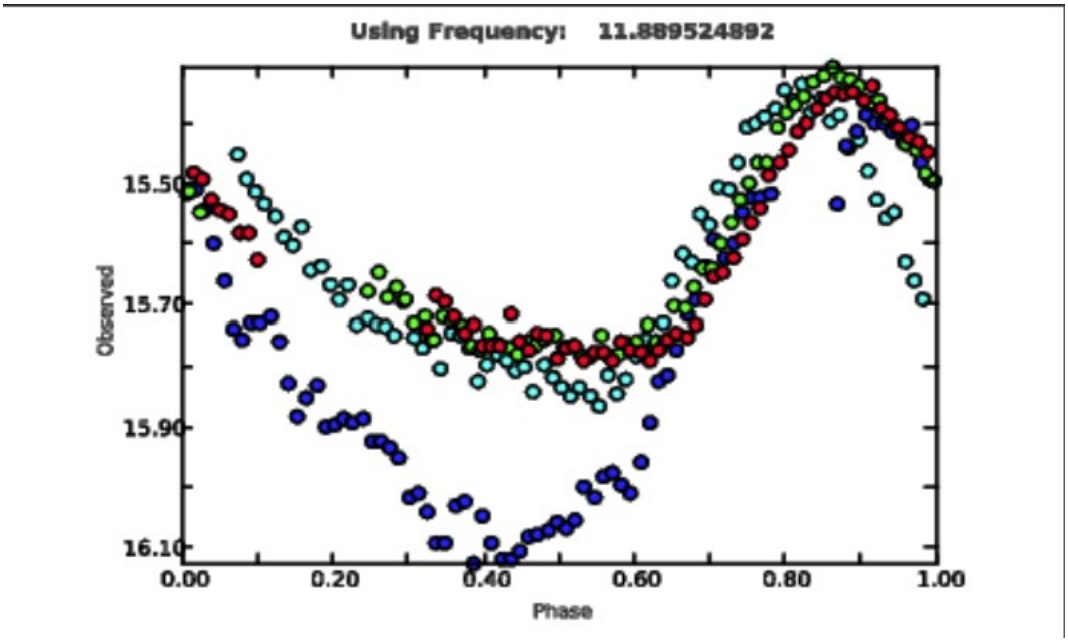

Figure 3.15 Phase diagram for ATLAS734

Figure 3.16 shows the phase diagram of ATLAS734 without the data from August 25, 2020. Figure 3.17 shows the phase diagram of ATLAS734 without the data from August 26, 2020. Figure 3.17 shows the phase diagram of ATLAS734 without the data from July 10, 2020. Figure 3.18 shows the phase diagram of ATLAS734 without the data from July 8, 2020. Each of these five diagrams have different frequencies. There is a huge frequency difference between Figure 3.15 and Figure 3.19. The frequency difference between these two diagrams is 1.022895473, which is a period difference of 0.977616 hours. As stated earlier, δ Scuti stars have a period of 1-2 hours. Since there is a 1 hour discrepancy between these two diagrams, that gives greater evidence that this object may not be a single period δ Scuti star. I have only come to conclusion with this object and that is that more data needs to be collected and analyzed to further conclude the type of star this object is. With my data, this star could be reclassified as a MATLAS object.

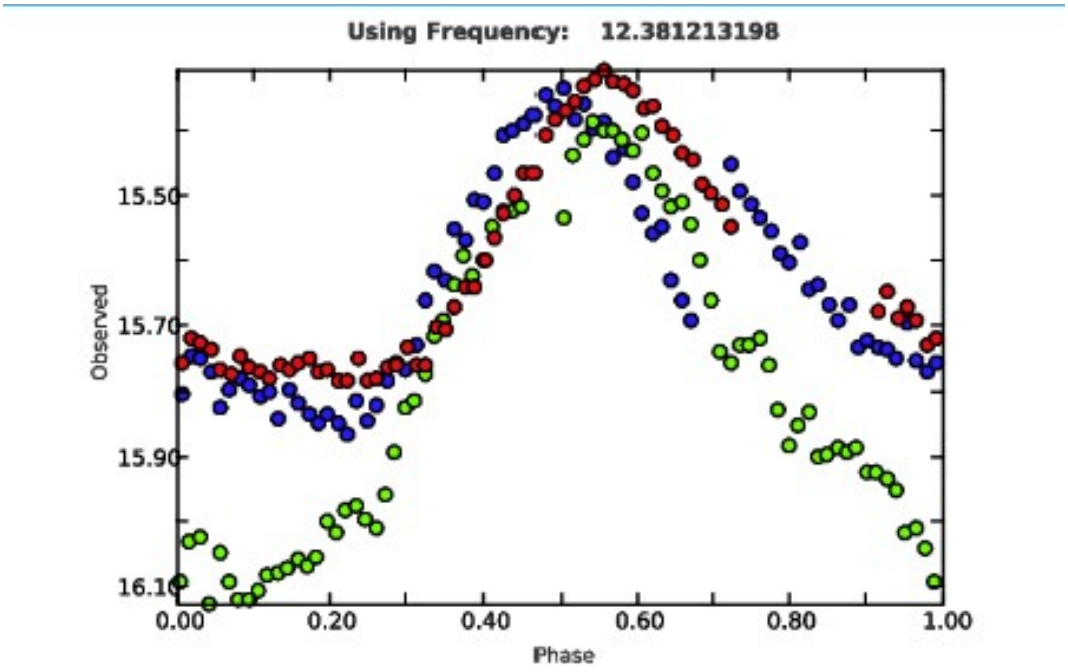

Figure 3.16 Phase diagram for ATLAS734 without August 25, 2020

3.3 Period Comparisons

The purpose of my research is to compare the published pulsation period of various ATLAS and MATLAS stars, found through the ATLAS Survey, with my observed pulsation period from data collected by DAO. Table 3.1 compares ATLAS published periods with my observed periods of ATLAS objects. I added in two other δ Scuti stars that I analyzed to show that there is a pattern. My observed periods match quite well to the ATLAS Survey's published periods. My pulsation periods for ATLAS388 and ATLAS411 are the most accurate to their published periods which is the reason that I presented them in this paper. The biggest difference (besides ATLAS734 which I talk about below) is from ATLAS818 with 8.2 minutes which is a little more than one tenth of an hour. This time difference is not anything to worry about, it is most likely due to the faintest of this star and the brightness of the objects surrounding this star. The difference between the published and observed period of ATLAS 368 is 4 minutes. This star was difficult to observe because it was next

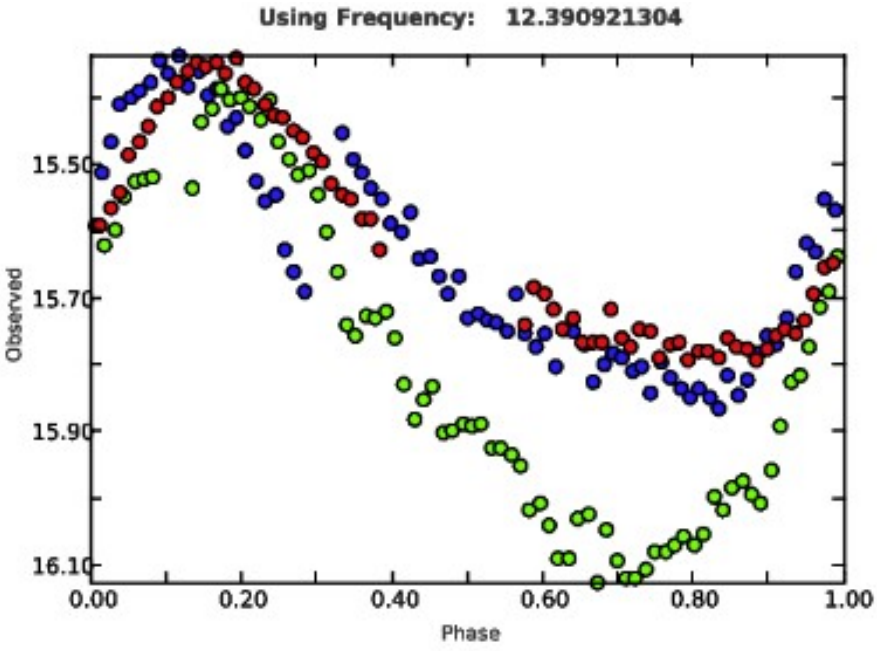

Figure 3.17 Phase diagram for ATLAS734 without August 26, 2020

Table 3.1. The observed periods and published periods for ATLAS objects.

Object	Observed Period days	Observed Period hours	Published Period days	Published Period hours	Difference days	Difference hours	Difference minutes
A368	0.08095	1.94299	0.07811	1.87468	0.00284	0.06830	4.09840
A388	0.07245	1.73889	0.07245	1.73887	9.484E-07	2.2762E-05	0.00136
A411	0.07377	1.77054	0.07377	1.77057	1.231E-06	2.9543E-05	0.00177
A818	0.07827	1.87865	0.07255	1.74120	0.00572	0.13745	8.24740

to a very bright object. Due to this bright object, the difference in periods is not surprising. Our conclusion is that the ATLAS Survey is quite good at finding pulsation periods for single period δ Scuti stars. Although this may bring up doubts due to ATLAS734, more δ Scuti stars found by ATLAS need to be observed so that we can come to a fair conclusion about the accuracy of the ATLAS Survey. After all, only a couple of single period variable stars were used in my study.

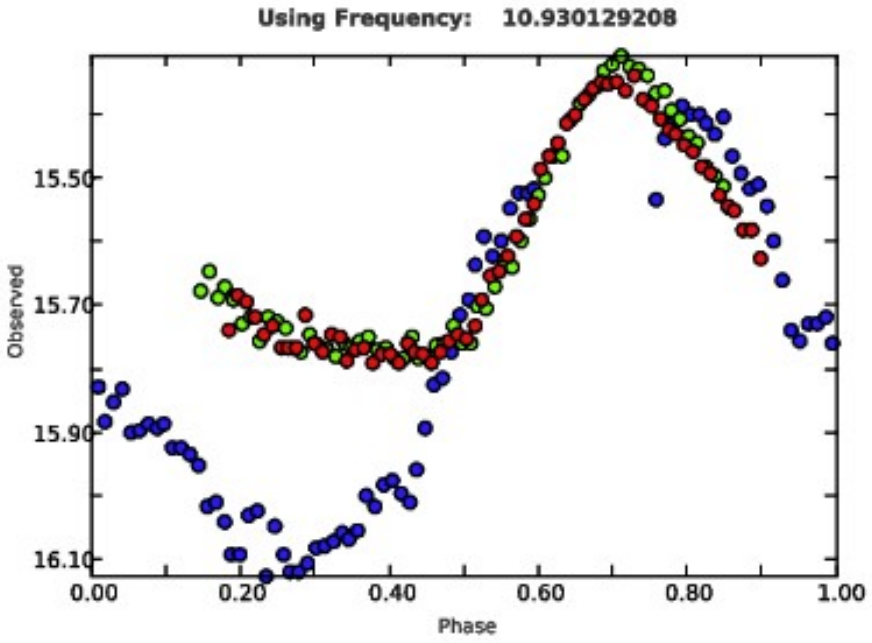

Figure 3.18 Phase diagram for ATLAS734 without July 10, 2020

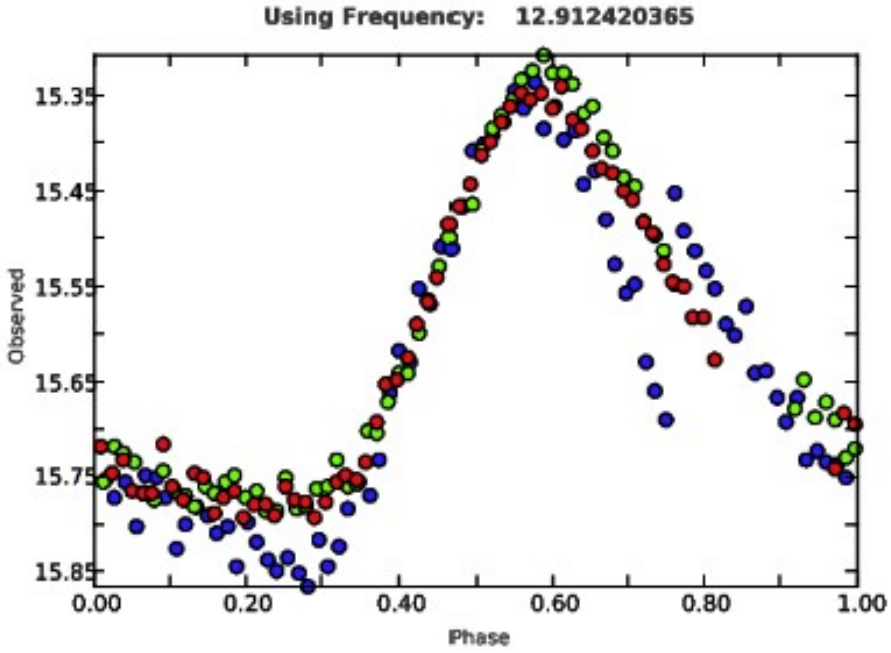

Figure 3.19 Phase diagram for ATLAS734 without July 8, 2020

Table 3.2. The observed periods and published periods for MATLAS objects.

Object	Observed Period days	Observed Period hours	Published Period days	Published Period hours	Difference days	Difference hours	Difference minutes
M355	0.07654	1.83714	0.25549	6.13188	0.17894	4.29473	257.683
M535	0.06653	1.59686	0.13306	3.19351	0.06652	1.59664	95.7986
M545	0.04324	1.03784	0.12974	3.11388	0.08650	2.07603	124.562
M549	0.06573	1.57769	0.17427	4.18255	0.10853	2.60485	156.291
M564	0.05666	1.35984	0.11349	2.72380	0.05683	1.36396	81.8376
M566	0.06012	1.44291	0.12023	2.88564	0.06011	1.44272	86.5634
M600	0.05582	1.33988	0.11835	2.84059	0.06252	1.50070	90.0421

Next, we will focus on the MATLAS stars. The MATLAS stars that I observed showed an unexpected trend. As you can see, in Table 3.2, my observed pulsation periods differ from the ATLAs Survey published periods by quite a few hours in some cases. When presenting my results to Dr. Hintz, we both noticed that, when comparing the Observed Period (hours) and Published Period (hours) columns, the relationship between them is a integer multiple. This is an interesting result and, honestly, quite confusing. Dr. Hintz and I guess that the ATLAS Survey had some difficulties analyzing the multiple periods found within each star. We are not sure why there are differences here or what could have caused it but we plan on contacting ATLAS with our observation results in hopes of provoking ATLAS to perform further observations on these objects. We assume, based on the number of stars I analyzed and this consistent trend, that other MATLAS published data may follow this trend. More MATLAS stars need to be observed to conclude that the ATLAS published data for MATLAS stars is off and that correct data needs to be available to the public to create accurate δ Scuti models.

Lastly, we will look at the ATLAS734 data. As you can see, in Table 3.3, the results for my measurements on ATLAS734 seem to be inconsistent. There is no trend in this data which proves

Table 3.3. ATLAS734 Observed and Published Periods.

Object	Observed Period days	Observed Period hours	Published Period days	Published Period hours	Difference days	Difference hours	Difference minutes
A734 (w/o A25)	0.08076	1.93842	0.07197	1.72732	0.00879	0.21109	12.6655
A734 (w/o A26)	0.08070	1.93690	0.07197	1.72732	0.00873	0.20957	12.5744
A734 (w/o J8)	0.09149	2.19576	0.07197	1.72732	0.01951	0.46843	28.1062
A734 (w/o J10)	0.07744	1.85867	0.07197	1.72732	0.00547	0.13134	7.88085
A734 (All)	0.08410	2.01852	0.07197	1.72732	0.01213	0.29120	17.47205

what we claimed before, however, keep in mind that July 10th was the outlier night in my set of data. When you look at the Differences (minutes) column (where it can be more easily seen) ATLAS734 (w/o J10) has the smallest difference between the published and observed periods. The difference is 7.9 minutes which lies beneath the maximum difference of 8.2 minutes from ATLAS818. This night does not necessarily prove that ATLAS734 is a multi periodic variable star, as there is no multiple integer trend here, but there is proof that this star does not act the way that single periodic stars do. That single night of data has us question the rest of the ATLAS objects that were found through the ATLAS Survey. Perhaps there are more ATLAS stars with similar data to this one but they have a title of an ATLAS or MATLAS star. Whatever the reason is, one thing is clear, that more data needs to be collected on this object. At this time, I have not analyzed anymore data on this object.

All of the results I have received has caused me to ponder on whether the ATLAS Survey data should be available to the public. My results prove that there should be some doubt in the ATLAS Survey data and that, perhaps, this data should not be trusted at all. I was only able to analyze a couple of these stars and there are already inconsistencies. We want data that can be trusted so that, when we start making models, we can say that we used accurate data. Inaccurate data means inaccurate models. The hope for this paper is to publish data that can be trusted so that, when δ Scuti models are made (hopefully by us in the near future), they are as accurate as possible.

List of Figures

List of Tables

Bibliography

[1] M. Farnir, A. Valentino, M. A. Dupret, and A. M. Broomhall, "Study with WhoSGlAd of the acoustic depth of the helium glitch across the seismic HR diagram and its impact on the inferred helium abundance," Monthly Notices of the Royal Astronomical Society (2023).

[2] J. L. Sanders and N. Matsunaga, "Hunting for C-rich long-period variable stars in the Milky Way's bar-bulge using unsupervised classification of Gaia BP/RP spectra," Monthly Notices of the Royal Astronomical Society **521,** 2745–2764 (2023).

[3] C. Latham, J. Kamenetzky, and M. T. Fitzgerald, "An Estimate of the Distance to AN Ser using an RR Lyrae Period-Luminosity Relationship," Research Notes of the AAS 7 (2023).

[4] V. V. Bobylev and A. T. Bajkova, "3D Kinematics of Classical Cepheids According to Gaia EDR3 Catalog," Research in Astronomy and Astrophysics 23 (2023).

[5] G. Michalska, Z. Kołaczkowski, R. Leiton, O. Szewczyk, K. Kinemuchi, and V. M. Kalari, "A CCD search for variable stars in the open cluster NGC 6611," Monthly Notices of the Royal Astronomical Society **520,** 5487–5505 (2023).

Index